Toughen and Strengthen Alginate Fiber by Incorporation of Polyethylene Glycol Grafted Cellulose Nanocrystals

Yaqi Wang
Wuhan Textile University
Hang Chen
Wuhan Textile University
Li Cui (cuili@wtu.edu.cn)
Wuhan Textile University - Yangguang Campus: Wuhan Textile University https://orcid.org/0000-0002-3648-3927
Chao Tu
Wuhan Textile University
Chao Yan
Wuhan Textile University

Research Article

Keywords: Alginate, Cellulose nanocrystals, Polyethylene glycol, Wet-spinning, Toughen, Strengthen

Posted Date: October 20th, 2021

DOI: https://doi.org/10.21203/rs.3.rs-898114/v1

Abstract

Alginate fibers have great potential in many applications, such as medical dressings, surgical sutures, and masks, etc. owing to their good biocompatibility and other properties. However, for alginate fibers prepared by wet spinning, the fibers have disadvantages such as low strength, poor toughness, and brittleness. Herein, a simple, scalable, and cost-effective blending spinning strategy was developed to produce the alginate composite fibers with excellent mechanical properties. Cellulose nanocrystals (CNCs) were incorporated directly in the wet spinning solution to improve its strength, wherein the CNCs were prepared from waste cotton fabrics. Polyethylene glycol (PEG) molecular chain was grafted onto the CNC surface to be used as a plasticizer while increasing the dispersibility of CNCs in alginate matrix. It was worth noting that modification of alginate fibers with PEG grafted cellulose nanocrystals (CNC-g-PEG) enhanced the tensile strength and elongation at break, simultaneously. In addition, the CNC-g-PEG modified alginate fibers exhibited improved salt tolerance and reduced water absorbency. This work may make high-value utilization of waste cotton fabrics, and pave the way for the development of high-performance, green alginate fibers.

1. Introduction

Sodium alginate, the raw material of alginate fibers, is a natural polysaccharide. Its molecule is composed of β-D-mannuronic acid (M) and α-L-guluronic acid (G) connected by 1-4 glycosidic bonds. Because of its good biocompatibility, natural degradability, water absorption, and non-toxicity, it is widely used in biomedicine, textile, and sewage treatment fields, such as medical wound dressings (Zheng et al. 2021). In the long run, the oil reserves on the earth are gradually decreasing, and the sustainable natural resources of bio-based fibers are more worthy of research by scholars than oil-based synthetic fibers (Ma et al. 2017).

Conventional pure alginate fibers prepared by wet spinning technology have poor mechanical properties because the wet spinning process conditions determine that there are fewer gaps in the supramolecular structure of alginate fibers (Potiwiput et al. 2019). When the external force is stretched, the fiber will break due to stress concentration. However, the crystallinity and orientation of alginate are low. The force between the macromolecules is weak, and the initial modulus is small. When a large external force acts on the alginate fiber, the macromolecular chain will relatively slip, which will also lead to the fiber fracture (Smyth et al. 2017). In a word, the structural characteristics of alginate fiber make it have the disadvantages of low strength, high brittleness, and poor toughness. It is easy to be squeezed and deformed during processing, production, and application, which affects its further application in medical, textile, and other fields.

In order to overcome these limitations, some nano, natural, synthetic polymers such as nanomaterials (nanocellulose) (Park et al. 2021), natural polymer materials (gelatin, chitosan) (Dong et al. 2006; Mikos et al. 1994), synthetic polymers (polyvinyl alcohol) (Fan et al. 2005), and other mixing was used to improve the mechanical properties and adsorption properties of the alginate fiber. Liu J et al. (2019)

reported that the breaking strength of alginate fiber can be significantly improved by the addition of CNCs (2 wt%) because the nano-size of CNCs makes it easier to diffuse into the alginate matrix and act as enhancers. Simultaneously, more hydrogen bonds can be formed between the alginate matrix and the hydroxyl groups on CNCs, which improves the stability of the macromolecular network structure and improves the fiber load capacity. However, in some hydrophobic or low-polar polymers, nano-cellulose is prone to agglomeration due to intermolecular hydrogen bonding, which greatly reduces the strengthening effect of nanocellulose (Musa et al. 2015). In our previous research, we found that CNCs were added as effective nucleating agents to the poly(L-lactic acid)/poly(D-lactic acid) (PDLA/PLLA) matrix to promote the mechanical properties and thermal stability of PLLA/PDLA composites films (Cao et al. 2021). However, the elongation at the break of these composites films is slightly decreased. In this regard, there are still some challenges in using CNCs to strengthen and toughen polymer materials, simultaneously. The modification of CNCs is an optional way to make it compatible and dispersed in the polymer matrix, so as to achieve a better enhancement effect (Lu et al. 2016; Sahlin et al. 2018). Ten et al. (2010) took 30% polyethylene glycol (PEG) as a compatibilizer to effectively increase the dispersibility of CNCs in a poly(hydroxybutyrate-co-hydroxyvalerate) matrix. The mechanical properties of the modified composite material have been significantly improved. PEG is a widely used high molecular polymer with good water solubility and good compatibility with many organic components and aliphatic polyesters such as PLLA (Pivsa-Art et al. 2016; Lai et al. 2004; Hu et al. 2003). It can effectively enhance the obdurability and tractility of polymer materials. Moreover, PEG has good biocompatibility, biodegradability, non-toxicity, and other characteristics, making it widely used in the fields of cosmetics, textiles, biomedicine, and food processing. (Min et al. 2015; Gui et al. 2012). In our study, PEG is chosen to modify CNCs by the grafting method. This way not only retains the excellent biodegradability and biocompatibility of nanocellulose but also improves the dispersion stability of CNCs in the alginate matrix. And, CNCs used in this research are obtained from waste cotton fabrics. (Cao et al. 2021) As is known to all, no investigation has ever been covered on this.

Here, we report a series of CNC-g-PEG modified alginate composite fibers prepared by wet spinning with CNC-g-PEG as a bifunctional enhancer into alginate fibers, in which the CNC fillers are used as green enhancers, and PEG molecular chain is used as a plasticizer while increasing the dispersibility of CNCs. The morphology, microstructure, and mechanical properties of the prepared alginate composite fibers were analyzed in detail. As expected, the incorporation of CNC-g-PEG can synergistically strengthen and toughen alginate fibers. The prepared alginate composite fibers are green biomass fibers, which have great application prospects in the field of medical dressings.

2. Experimental

2.1 Materials

Sodium alginate (SA, viscosity:700 mPa·s, M/G ratio =1:1.5) was provided by Qingdao Bright Moon Seaweed Group Co., Ltd. (Shandong, China). Polyethylene glycol (PEG, $\overline{Mn}$ =1000, 2000, 4000) was

purchased from Sinopharm Chemical Reagent Co., Ltd, China. Other chemical reagents were purchased from Sinopharm Chemical Reagent Co., Ltd. Phosphate buffered saline (PBS, pH=7.2-7.4, 0.01 M, Beijing Solarbio Science & Technology Co., Ltd.) was purchased and directly used without further purification.

2.2 Extraction and modification of CNCs and its chemical grafting of PEG with different molecular weights

CNCs were prepared from waste cotton fabric according to our previous methods. (Cao et al. 2021)

To prepare the oxidized CNCs, NaBr and TEMPO were dissolved in a small amount of deionized water and then poured into the CNC suspension after ultrasonic treatment. The pH value of the suspension was adjusted to 10.2 with the dilute hydrochloric acid solution, NaClO was added with slow stirring, and then the pH value of the reaction system was maintained at 10-10.5 with dilute NaOH solution. After fully reacting for 3 hours, about 5 mL of ethanol was added to terminate the reaction. The oxidation product was thoroughly filtered and washed with deionized water to neutrality (Yao et al. 2015). The oxidized CNCs (OCNCs) will be used in the subsequent experiments.

About 10 g of PEG with different molecular weights (PEG1000, PEG2000, PEG4000) and 0.5 g of CNCs were placed in an Erlenmeyer flask and stir vigorously. Then 0.1 ml of Sn $(Oct)_2$ was added to the reaction system. The reactant solution was heated to 90°C for 6 h under stirring at 800r/min. Lastly, ethanol was added to terminate the reaction. The remaining Sn $(Oct)_2$ and ungrafted PEG in the product were removed by centrifugation The centrifuged product was dialyzed for one week and then freeze-dried to obtain the graft copolymer. The products were designed as CNC-g-PEGX (X refers to the molecular weight of PEG). In addition, the grafting rate of PEG measured by the weighing method was 31.3%.

2.3 Preparation of the alginate composite fibers

In our previous work, alginate composite fibers containing CNCs (8 wt%) showed better performance. So in this study, the content of CNCs or CNC-g-PEG in alginate fibers was fixed at 8 wt%. Alginate composite fibers were prepared by wet spinning. Firstly, CNC or CNC-g-PEG powder was dispersed in water by sonication method for one hour. Then 4 wt% sodium alginate was added with stirring at 400 r/min for 6 hours at 45°C until a homogeneous mix of spinning dope was acquired. The spinning dope was injected into the coagulation bath of the $CaCl_2$ aqueous solution through a self-made wet spinning machine. After the spinning was completed, the formed fiber was cleaned with deionized water to remove NaCl and $CaCl_2$ on the fiber surface, and then continuously immersed in alcohol with increasing volume fractions (20 vol.%, 30 vol.%, and 50 vol.%) to remove the water inside the fibers, and finally dried and collected under natural conditions. The alginate composite fibers contained CNCs and CNC-g-PEGX were recorded CNC/Alginate fibers and CNC-g-PEGX/Alginate fibers (X represented the molecular weight of PEG), respectively. The diagram of the total preparation process is shown in Fig. 1.

2.4 *Measurement and characterization*

2.4.1 Fourier transform infrared (FTIR) measurement

The FTIR spectra were recorded on a TENSOR-27 type Fourier transform infrared spectrometer (Bruker Co, USA) with a resolution of 2 cm^{-1} in the wavenumber range of 400-4000 cm^{-1}. The samples were prepared for analysis by grinding the dry blends with KBr and compressing the mixtures to form sheets.

2.4.2 Scanning electron microscope (SEM)

The morphology of the prepared fibers was observed using a JEOL JSM-5600LV scanning electron microscope (SEM, Japan). The surfaces of the samples were subjected to a 10 nm gold spray treatment.

2.4.3 Powder X-ray diffraction analysis (XRD)

The crystal structures of the samples were conducted using a Riguaku X-ray diffractometer (Ultima VI, Japan) with a Cu Kα radiation (k = 0.15418 nm) over a 2θ range of 5-80° with a step size of 0.05°. The degree of crystallinity (X_c) was calculated according to the deconvolution method by using the Eq. (1):

$$X_c = A_c/(A_c + A_a)$$

1

where A_c represents area under crystalline peaks and A_a is area under amorphous region.

2.4.4 Mechanical property

The mechanical properties of prepared samples were tested according to GB/T 14337-2008 on an XQ-1 fiber tensile tester (Shanghai New Fiber Instrument Co., Ltd, China) at a crosshead speed of 10 mm·min^{-1} at 20 ℃ and 40 % relative humidity. At least 20 independent samples of each specimen were tested and averaged.

2.4.5 Water absorbency

The fiber samples were dried at 50 ℃ in a vacuum dryer for 24 h and weighed (W_0). Then, the dried sample was immersed in distilled water to swell at 25°C. After swelling equilibrium, the samples were taken out and weighted (W_t) after removing the excess water on the surface by filter paper. The water absorbency was calculated as follows:

$$\text{Water absorbency}(\%) = \frac{\mathrm{W_t\text{-}W_0}}{\mathrm{W_0}} * 100\%$$

2

The results were expressed as an average value from at least three tests.

2.4.6 Salt tolerance

The fiber samples were treated in a series of NaCl solutions of different concentrations (10 g/L, 15 g/L, 20 g/L, 25 g/L, 30 g/L) for 1 h and taken out. When there were no drops on the fiber surface, the weight was weighed. Then the fiber samples were dried at 50 ℃ in a vacuum dryer for 24 h and weighed. The swelling degree (S) of the fiber was calculated according to Eq. (3):

$$S(\%)=\frac{W_s\text{-}W_d}{W_d}*100\%$$

3

where W_s was the sample's weight after absorbing NaCl and W_d was the sample's weight after drying. The final result was the average of 3 sets of data.

2.4.7 Biodegradability

The in vitro degradation of alginate fiber was carried out using phosphate-buffered saline (PBS). About 150 ml of PBS solution was added to a 250 ml Erlenmeyer flask, sealed, and sterilized for 30 minutes. Then about 0.5 g of dry sample was added and shook well. The Erlenmeyer flask containing PBS and sample fibers was placed at about 37°C. The sample fiber was collected on the 5th, 10th, 15th, 20th, 25th, and 30th days, and was washed with distilled water several times to remove the salt. The precipitate was dried in a vacuum to a constant weight and then weighed. The weight loss rate of the sample fiber was calculated according to Eq. (4):

$$W(\%)=\frac{(M_0\text{-}M_1)}{M_0}*100\%$$

4

where W was the weight loss percentage of the sample, and M_0 (g) and M_1 (g) were the dry sample weight before and after degradation, respectively.

3. Results And Discussion

3.1 Morphology and stability of CNCs and CNC-g-PEG

As shown in Fig. 2 (a), CNCs obtained from waste cotton fabrics displayed rod-shaped nanocellulose with a high aspect ratio. Fig. 2 (b) showed that the CNC and CNC-g-PEG suspensions were in light blue and no visible sedimentation was observed at the bottom of glass bottles after ultrasonication (0 day). However, 30 days later, a large number of CNCs presented obvious agglomeration, while good stability for CNC-g-PEG suspension was remained. The CNCs prepared by hydrolysis of sulfuric acid was electrostatically stable due to the negatively-charged sulfate (SO_4^{2-}) groups on the surface of CNCs (Habibi et al. 2010). However, for CNC-g-PEG, the steric hindrance effect of PEG molecular chain on the CNC surface could replace the electrostatic stabilization to prevent agglomeration and precipitation. And PEG, as a hydrophilic and flexible long chain, could better promote CNC-g-PEG suspension to form a stable solution with good dispersion performance (Zheng et al. 2021). Furthermore, the additional COO^- groups generated from the selective oxidation of TEMPO also played a positive role in the dispersibility of CNC-g-PEG suspension (Ma et al. 2017). The good stability of CNC-g-PEG suspensions could be preserved for several months by putting at low temperature.

3.2 Typical chemical structures and properties of CNCs and CNC-g-PEG

The FT-IR spectra of the obtained CNCs, OCNCs, PEG, and CNC-g-PEG2000 are shown in Fig. 3. At about 3400 cm^{-1}, the intensity of the -OH stretching vibration peak of OCNCs was weaker than that of CNCs, indicating that part of the hydroxyl groups on the CNC surface had reacted. The peak intensity of OCNCs at 1640 cm^{-1} increased, which corresponded to the C=O bending vibration of the carboxyl group. This proved that the CNCs had been successfully oxidized by TEMPO. In particular, the new appeared peak at about 1738 $cm^{-1}$was attributed to the carbonyl vibration, because the carboxyl group on CNCs was successfully esterified by the hydroxyl group on PEG during the hydrolysis process (Gu et al. 2016). Therefore, the FT-IR results proved that PEG was successfully grafted onto the CNC surface.

Figure 4 is the XRD spectra of CNCs, CNC-g-PEG, PEG and the waste cotton. Three characteristic diffraction peaks were observed at 2θ = 14.8°, 16.5°, 22.7°, corresponding to $(1\bar{1}0)$, (110), (200) crystal planes of cellulose I crystals crystallized in a monoclinic pattern (Yu et al. 2014). The crystal structure of the waste cotton and prepared CNCs retained the cellulose I crystals structure of natural biomass cellulose. After grafting reaction, CNC-g-PEG showed characteristic peaks of PEG and CNCs, which indicated that PEG was successfully grafted to the CNC surface and the original crystal type and main crystal structure of CNC-g-PEG were still maintained.

3.3 Morphology of the alginate composite fibers

The SEM images (see Fig. 5) showed the surface of the fibers had obvious grooves and linear structures, which were caused by uneven shrinkage due to the different removal rate of a large amount of solvent between the surface and interior of the fiber during the coagulation and molding process (Zhang et al. 2018). Compared with pure alginate fibers, CNC-g-PEG/Alginate fibers exhibited more and deeper grooves on the surface. This was attributed to the formation of hydrogen bonds between CNCs and alginate macromolecules in the alginate fiber, which increased the number of wrinkles on the fiber surface. In addition, the tensile fracture cross-section of alginate fibers and CNC/Alginate fibers were relatively smooth. This indicated that their ability to resist crack propagation was weak, and the fiber might undergo brittle fracture. However, after the addition of CNC-g-PEG, the roughness of the fractured cross-section increased significantly. Moreover, this improvement increased with the increase of PEG molecular weight. There were more and more irregular zigzag stripes on the fractured cross-section of modified alginate fibers. This was the main feature of the matrix's transformation from brittleness to plastic deformation (Terentyev et al. 2019), indicating that the ability of modified fiber to resist crack propagation had been improved.

3.4 Aggregated structure of the alginate composite fibers

Figure 6(a) shows the XRD spectra of alginate fibers, CNCs, and CNC-g-PEG modified alginate fibers. Alginate fibers had a broad diffraction peak near 2θ = 13.2°and 22.6°, which were assigned to (110) plane from polyguluronate unit (G),

(200) plane from polymannuronate (M) (Sundarrajan et al. 2012). The characteristic peaks of pure alginate fibers were wide and diffuse, confirming that pure alginate fibers themselves had weak crystalline properties. After the addition of CNCs or CNC-g-PEG, the intensity of the diffraction peak of CNC/Alginate fibers or CNC-g-PEG/Alginate fibers increased significantly, and the peak shape became narrower. The characteristic diffraction peak of alginate fibers at 2θ = 13.2° showed a higher diffraction peak intensity and a narrower peak shape. It could be seen from Fig. 6(b) that compared with pure alginate fibers, the crystallinity of the modified alginate composite fibers increased. This was because CNCs and CNC-g-PEG could play the role of heterophase nucleation. At the same time, CNCs and CNC-g-PEG reacted with the hydroxyl group on the macromolecular chain. More hydroxyl groups were introduced into the alginate fibers. The hydrogen bonding force between the molecules of the modified alginate fibers was enhanced and resulted in the improvement of the regularity and order of the molecular chain. So the degree of crystallinity of alginate composite fiber was improved to a greater extent.

3.5 Mechanical properties of the alginate composite fibers

The breaking strength and elongation at the break of alginate fibers and alginate composite fibers are shown in Fig. 6(c). As expected, pure alginate fibers had the lowest tensile strength value. The tensile strength of alginate composite fibers can be significantly improved by adding CNCs and CNC-g-PEG. In this blending system, CNCs and PEG played the role of reinforcing agent and compatibilizer/toughing agent in alginate composite fibers, respectively. When CNCs (8 wt%) was added to the sodium alginate spinning solution, the tensile strength of the alginate composite fibers reached the maximum, but its elongation at break was even worse than pure alginate fibers. However, it was worth noting that incorporating 8 wt% CNC-g-PEG with different molecular weights, the elongation at break and tensile strength of alginate composite fibers were both higher than that of pure alginate fibers. When the PEG molecular weight increased, the tensile strength was gradually decreased, instead, the elongation at break was increased.

Increased crystallinity, intermolecular force, and regularity of macromolecular chain arrangement could promote the improvement of fiber mechanical properties to a certain extent. Compared with CNC-g-PEG/Alginate fibers, at the same loading levels, the CNCs showed greater enhancement in tensile strength under the same amount. Higher crystallinity and good interface adhesion (hydrogen bond) of alginate composite fibers were contributed to improving their tensile strength. In addition, the CNC nanoparticles dispersed in the alginate matrix could serve as the stress concentration center and induced the generation of silver stripes and shear bands to consume a large amount of energy. Nevertheless, the grafted PEG molecular chains would instead hydroxyl groups on the CNC surface. The hydrogen bonds between CNCs and alginate chains were reduced. At the same time, CNC-g-PEG macromolecular chains contained flexible PEG side chains, which increased the distance between macromolecules and improved the mobility of molecular chains. The grafted PEG chain could be used as a bridge to enhance the interface characteristics/adhesion between CNCs and the alginate matrix. It was beneficial to transfer stress and strain of the alginate chains along the tensile direction hauled by the CNCs during the stretching process (Zhang et al. 2015). Thereby the toughness of the alginate composite fibers had been highly improved.

The plasticization effect of CNC-g-PEG with a larger PEG molecular weight also speeded up the mobility of the alginate chains along the tensile direction to enhance the toughness of the alginate fibers. Therefore, comprehensive evaluation of tensile strength and elongation at break properties, the addition of CNC-g-PEG2000 had the best effect of toughening and strengthening for the alginate composite fibers.

3.6 Biodegradability of the alginate composite fibers

The biodegradation behavior of prepared alginate composite fibers is shown in Fig. 7(a). All samples were immersed in PBS for 30 days. All fibers were being degraded over time and the weight loss was increased with the immersion time. The biodegradability of pure alginate fibers reached to 68% after 30 days. This was attributed to the hydrolysis of b-1,4 glycoside bond in alginate molecule. Due to the biodegradable rate of CNCs was lower than that of alginate (Cui et al. 2020; Doh et al. 2020), so when CNCs or CNC-g-PEG were added to the alginate matrix, the degradation of fibers became difficult. Therefore, it could be concluded from the results that the incorporation of CNCs or CNC-g-PEG in alginate matrix decreased the biodegradability of fibers. Overall it had a weaker effect on the degradation performance of alginate composite fibers.

3.7 Water absorbency of the alginate composite fibers

Alginate fibers have many hydrophilic groups (e.g. hydroxyl and carboxyl groups) that can combine with water molecules to form hydrogen bonds. In addition, the alginate fibers have many tiny voids which are generated in the wet spinning process. So alginate fibers had excellent moisture absorption capacity (Jabeen et al. 2016). As shown in Fig. 7(b), all of the fibers exhibited good water absorbency properties. The water absorbency of all alginate composite fibers was gradually decreased with the addition of CNCs or CNC-g-PEG. The water absorbency of alginate composite fibers was reduced by 19.7% after adding CNCs. Meanwhile, the reductions for the CNC-g-PEG1000/Alginate fibers, CNC-g-PEG2000/Alginate fibers, CNC-g-PEG4000/Alginate fibers were greater than that of CNC/Alginate fibers, which were reduced by 41.5%, 36%, 29.1%, respectively. This might be due to the relatively powerful interfacial interaction between CNC-g-PEG and alginate molecule, resulting in an increase in the crystallinity of the composite fibers and an increase in the tortuosity of the transport path for small molecules to diffuse through the alginate matrix (See Fig. 7(c)).

3.8 Salt tolerance property

The preparation of alginate fiber is a reversible process. When the content of Ca^{2+} is high, Na^{+} in alginate will be replaced to form crosslinking structure to coagulation. But, when there is too much Na^{+}, it will replace Ca^{2+} to gelation inversely (Chen et al. 2021). As shown in Fig. 8, the swelling degree of pure alginate fiber gradually increased and even dissolved as the concentration of NaCl solution increased. This was because as the concentration increased, Na^{+} would enter the fiber macromolecules to exchange with more Ca^{2+}. At the same time, more water molecules were introduced, which made the dissociation effect of water molecules became greater, eventually, the fibers dissolved. For alginate fibers modified by CNCs or CNC-g-PEG, the physical cross-linking between CNCs and alginate fibers prevented Na^{+} in NaCl solution from entering the fiber, destroying the "egg-box" structure of the fibers. It also prevented water

molecules from entering the fiber, reducing the dissociation effect (Chan and Neufeld 2009). However, as the concentration of Na^+ increased, a small part of Na^+ entered the fiber to exchange with Ca^{2+}, and the swelling degree of CNC/Alginate fibers and CNC-g-PEG/Alginate fibers gradually increased.

Conclusion

Alginate composite fibers blended with CNCs or CNC-g-PEG with various PEG molecular weights were successfully prepared through wet spinning. Compared to CNCs, CNC-g-PEG showed better interfacial compatibility with alginate fibers due to its steric hindrance. The tensile strength of alginate fibers reached a maximum value with the addition of 8 wt% CNCs, but its elongation at break was even worse than pure alginate fibers. However, the CNC-g-PEG showed a slightly lower reinforcing effect on tensile strength for alginate fibers than CNCs under the same amount of addition, while as the molecular weight of the grafted PEG increased, the elongation at break gradually reached 17.8%. Therefore, the CNC-g-PEG nanofillers showed positive effects on toughening and strengthen alginate composite fibers. Moreover, its toughening effect was enhanced by grafting a larger molecular weight of PEG into the CNC surface. Furthermore, the addition of CNCs and CNC-g-PEG reduced the water absorbency and improved the salt tolerance of the alginate composite fiber. In addition, compared with the alginate fibers, the biodegradability of CNC/Alginate fibers and CNC-g-PEG/Alginate fibers is slightly reduced. Such green composite fibers with excellent performance can be regarded as new materials in the field of medical textiles.

Declarations

Conflict of interest

The authors declare that they do not have any conflict of interest in submission of this manuscript.

Declaration of interests

✓ The authors declare that they have no known competing financial interests or personal relationships that could have appeared to influence the work reported in this paper.

The authors declare the following financial interests/personal relationships which may be considered as potential competing interests:

References

1. Cao X, Wang Y, Chen H et al (2021) Preparation of different morphologies cellulose nanocrystals from waste cotton fibers and its effect on PLLA/PDLA composites films. Compos B Eng 217:108934. https://doi.org/10.1016/j.compositesb.2021.108934

2. Chan AW, Neufeld RJ (2009) Modeling the controllable pH-responsive swelling and pore size of networked alginate based biomaterials. Biomaterials 30(30):6119-6129. https://doi.org/10.1016/j.biomaterials.2009.07.034
3. Chen Z, Song J, Xia Y et al. (2021) High strength and strain alginate fibers by a novel wheel spinning technique for knitting stretchable and biocompatible wound-care materials. Mat Sci Eng C 127:112204. https://doi.org/10.1016/j.msec.2021.112204
4. Cui L, Hu JJ, Wang W et al (2020) Smart pH response flexible sensor based on calcium alginate fibers incorporated with natural dye for wound healing monitorin. Cellulose 27:6367-6381 https://doi.org/10.1007/s10570-020-03219-1
5. Doh H, Dunno KD, Whiteside WS (2020) Cellulose nanocrystal effects on the biodegradability with alginate and crude seaweed extract nanocomposite films. Food Biosci 38(12):100795. https://doi.org/10.1016/j.fbio.2020.100795
6. Dong Z, Wang Q, Du Y (2006) Alginate/gelatin blend films and their properties for drug controlled release. J Membrane Sci 280:37-44. https://doi.org/10.1016/j.memsci.2006.01.002
7. Fan LH, Du YM, Wang XH, Huang RH, Zhang LN, Hu L (2005) Preparation and characterization of alginate/poly(Vinyl Alcohol) blend fibers. Macromol Sci A 42:41-50. https://doi.org/10.1081/MA-200040956
8. Gu M, Jiang C, Liu D et al (2016) Cellulose Nanocrystal/Poly (ethylene glycol) Composite as an Iridescent Coating on Polymer Substrates: Structure-Color and Interface Adhesion. ACS Appl Mater Inter 8(47):32565-32573. https://doi.org/10.1021/acsami.6b12044
9. Gui Z, Xu Y, Gao Y et al (2012) Novel polyethylene glycol-based polyester-toughened polylactide. Mater Lett 71:63-65 https://doi.org/10.1016/j.matlet.2011.12.045
10. Habibi Y, Lucia LA, Rojas OJ (2010) Cellulose nanocrystals: chemistry, self-assembly, and applications. Chem Rev 110(6):3479-500. https://doi.org/10.1021/cr900339w
11. Hu Y, Hu YS, Topolkaraev V et al (2003) Aging of poly(lactide)/poly(ethylene glycol) blends. Part 2. Poly(lactide) with high stereoregularity. Polymer 44:5711-5720. https://doi.org/10.1016/S0032-3861(03)00615-3
12. Jabeen S, Maswal M, Chat OA et al. (2016) Rheological behavior and Ibuprofen delivery applications of pH responsive composite alginate hydrogels. Colloids Surf B 139:211-218. https://doi.org/10.1016/j.colsurfb.2015.12.013
13. Lai WC, Liau WB, Lin TT (2004) The effect of end groups of PEG on the crystallization behaviors of binary crystalline polymer blends PEG/PLLA. Polymer 45:3073-3080. https://doi.org/10.1016/j.polymer.2004.03.003
14. Liu J, Zhang R, Ci MY et al (2019) Sodium alginate/cellulose nanocrystal fibers with enhanced mechanical strength prepared by wet spinning. J Eng Fiber Fabr 19:1-7. https://doi.org/10.1177/1558925019847553
15. Lu F, Yu H, Yan C et al (2016) Polylactic acid nanocomposite films with spherical nanocelluloses as efficient nucleation agents: effects on crystallization, mechanical and thermal properties. RSC Adv

6(51):46008-46018. https://doi.org/10.1039/C6RA02768G

16. Ma X, Li R, Zhao X et al (2017) Biopolymer composite fibers composed of calcium alginate reinforced with nanocrystalline cellulose. Compos Part A-Appl S 96:155-163. https://doi.org/10.1016/j.compositesa.2017.02.021
17. Mikos AG, Thorsen AJ, Czerwonka LA et al (1994) Preparation and characterization of poly (l-lactic acid) foams. Polymer 35:1068-1077. https://doi.org/10.1016/0032-3861(94)90953-9
18. Min X, Fang M, Huang Z (2015) Enhanced thermal properties of novel shape-stabilized peg composite phase change materials with radial mesoporous silica sphere for thermal energy storage. Sci Rep 5:12964. https://doi.org/10.1038/srep12964
19. Musa RK, Vahid K (2015) Effect of cellulose nanocrystals (CNC) on rheological and mechanical properties and crystallization behavior of PLA/CNC nanocomposites. Carbohydr Polym 123:105-114 https://doi.org/10.1016/j.carbpol.2015.01.012
20. Park JS, Park CW, Han SY et al (2021) Preparation and properties of wet-spun microcomposite filaments from various CNFs and alginate. Polymers 13(11):1709 https://doi.org/10.3390/polym13111709
21. Pivsa-Art W, Fujii K, Nomura K et al (2016) The effect of poly(ethylene glycol) as plasticizer in blends of poly(lactic acid) and poly(butylene succinate). J Appl Polym Sci 133:430-444. https://doi.org/10.1002/app.43044
22. Potiwiput S, Tan HP, Yuan GL et al (2019) Dual-crosslinked alginate/carboxymethyl chitosan hydrogel containing in situ synthesized calcium phosphate particles for drug delivery application. Mater Chem Phys 241:122354. https://doi.org/10.1016/j.matchemphys.2019.122354
23. Sahlin K, Forsgren L, Moberg T, et al (2018) Surface treatment of cellulose nanocrystals (CNC): effects on dispersion rheology. Cellulose 25(1):331-345. https://doi.org/10.1007/s10570-017-1582-5
24. Smyth M, Rader C, Bras J et al (2017) Characterization and mechanical properties of ultraviolet stimuli-responsive functionalized cellulose nanocrystal alginate composites. J Appl Polym Sci 135:45857. https://doi.org/10.1002/app.45857
25. Sundarrajan P, Eswaran P, Marimuthu A et al (2012) One Pot Synthesis and Characterization of Alginate Stabilized Semiconductor Nanoparticles. B Korean Chem Soc 33(10):3218-3224. https://doi.org/10.5012/bkcs.2012.33.10.3218
26. Ten E, Turtle J, Bahr D et al (2010) Thermal and mechanical properties of poly(3-hydroxybutyrate-co-3hydroxyvalerate)/cellulose nanowhiskers composites. Polymer 51:2652-2660. https://doi.org/10.1016/j.polymer.2010.04.007
27. Terentyev D, Riesch J, Dubinko A et al (2019) Fracture surfaces of tungsten wires used in fiber-reinforced plasma facing components: Effect of potassium doping and high temperature annealing. Fusion Eng Des 146:991-994 https://doi.org/10.1016/j.fusengdes.2019.01.137
28. Yao WR, Xu QH, Jin LQ et al (2015) Effects of TEMPO/NaBr/NaClO oxidation of nanocrystalline cellulose on its properties. Chem Ind Forest Prod 35:31-37. 10.3969/j.issn.0253-2417.2015.02.005

29. Yu H, Yan C, Lei X et al (2014) Novel approach to extract thermally stable cellulose nanospheres with high yield. Mater Lett 131(15):12-15. https://doi.org/10.1016/j.matlet.2014.05.159
30. Zhang C, Salick MR, Cordie TM et al (2015) Incorporation of poly(ethylene glycol) grafted cellulose nanocrystals in poly(lactic acid) electrospun nanocomposite fibers as potential scaffolds for bone tissue engineering. Mat Sci Eng C 49:463-471. https://doi.org/10.1016/j.msec.2015.01.024
31. Zhang R, Guo J, Liu Y et al (2018) Effects of sodium salt types on the intermolecular interaction of sodium alginate/antarctic krill protein composite fibers. Carbohydr Polym 189:72-78. https://doi.org/10.1016/j.carbpol.2018.02.013
32. Zheng T, Clemons CM, Pilla S (2021) Grafting PEG on cellulose nanocrystals via polydopamine chemistry and the effects of PEG graft length on the mechanical performance of composite film. Carbohydr Polym 12:118405. https://doi.org/10.1016/j.carbpol.2021.118405
33. Zheng Y, Sun Y, Cui Y et al (2021) Superhydrophobic and flame-retardant alginate fabrics prepared through a one-step dip-coating surface-treatment. Cellulose 28:5973-5984 https://doi.org/10.1007/s10570-021-03890-y

Figures

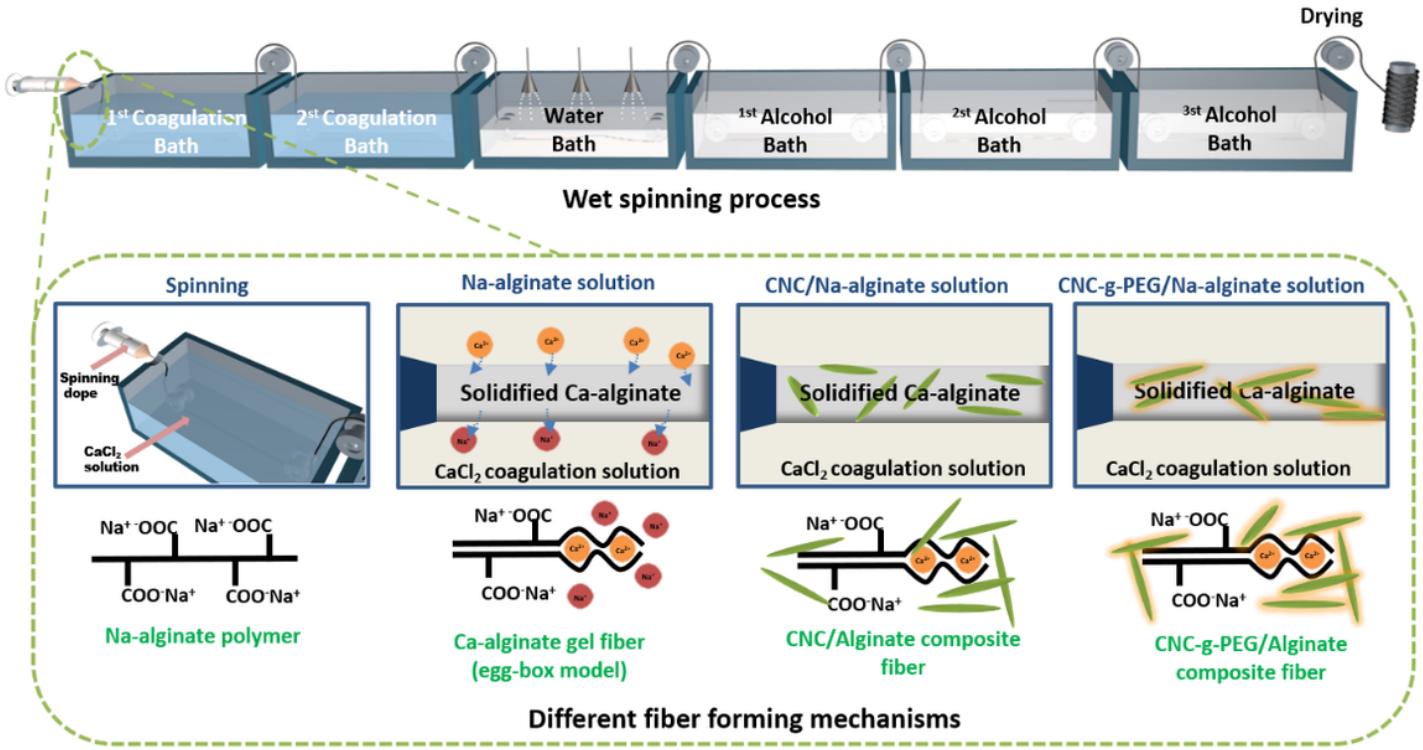

Figure 1

Preparation route of the alginate composite fibers

Figure 2

SEM images of CNCs from waste cotton fabrics (a), digital pictures of CNCs and CNC-g-PEG (b)

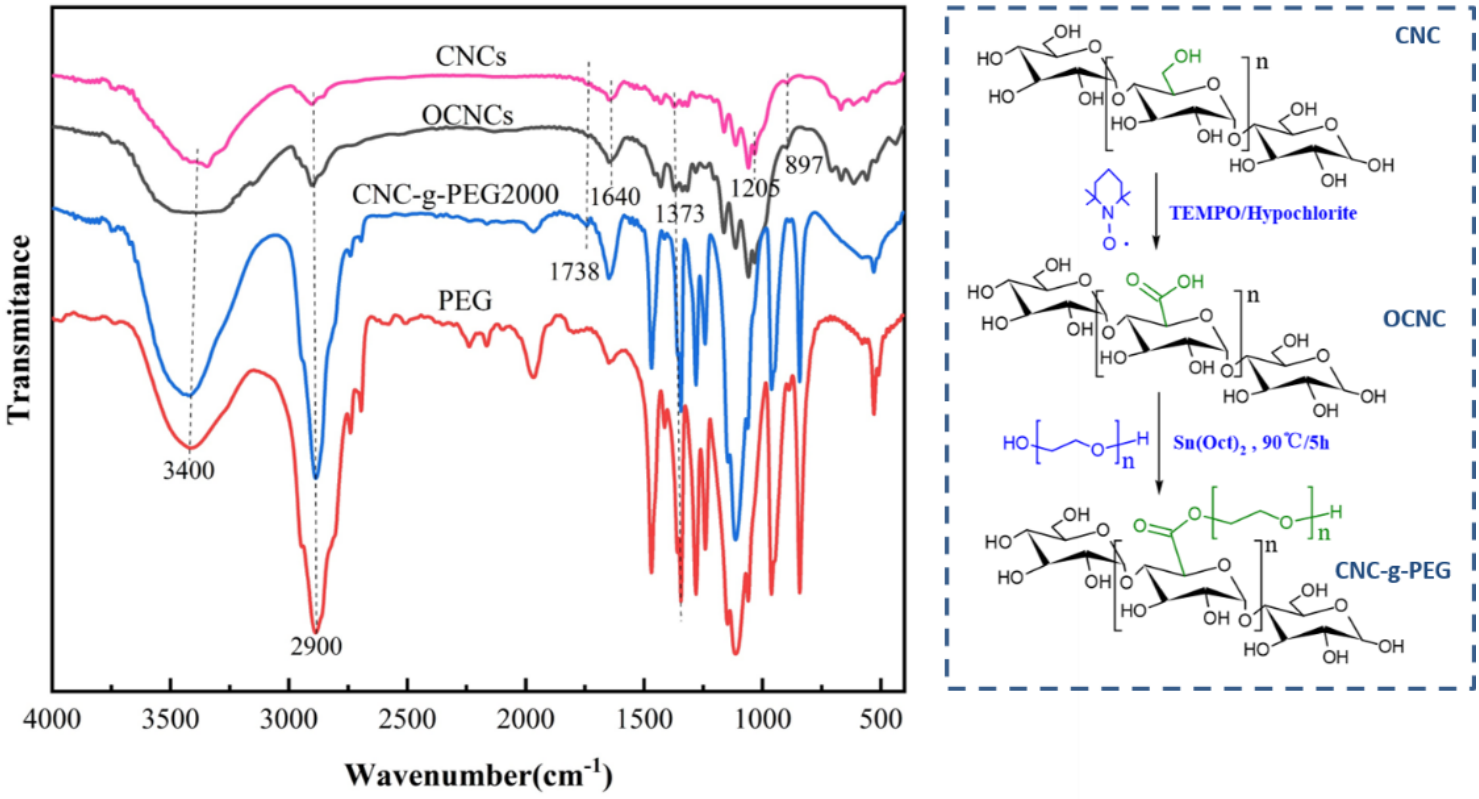

Figure 3

FTIR spectra of PEG, CNCs, OCNCs and CNC-g-PEG2000, and illustration of grafting reaction

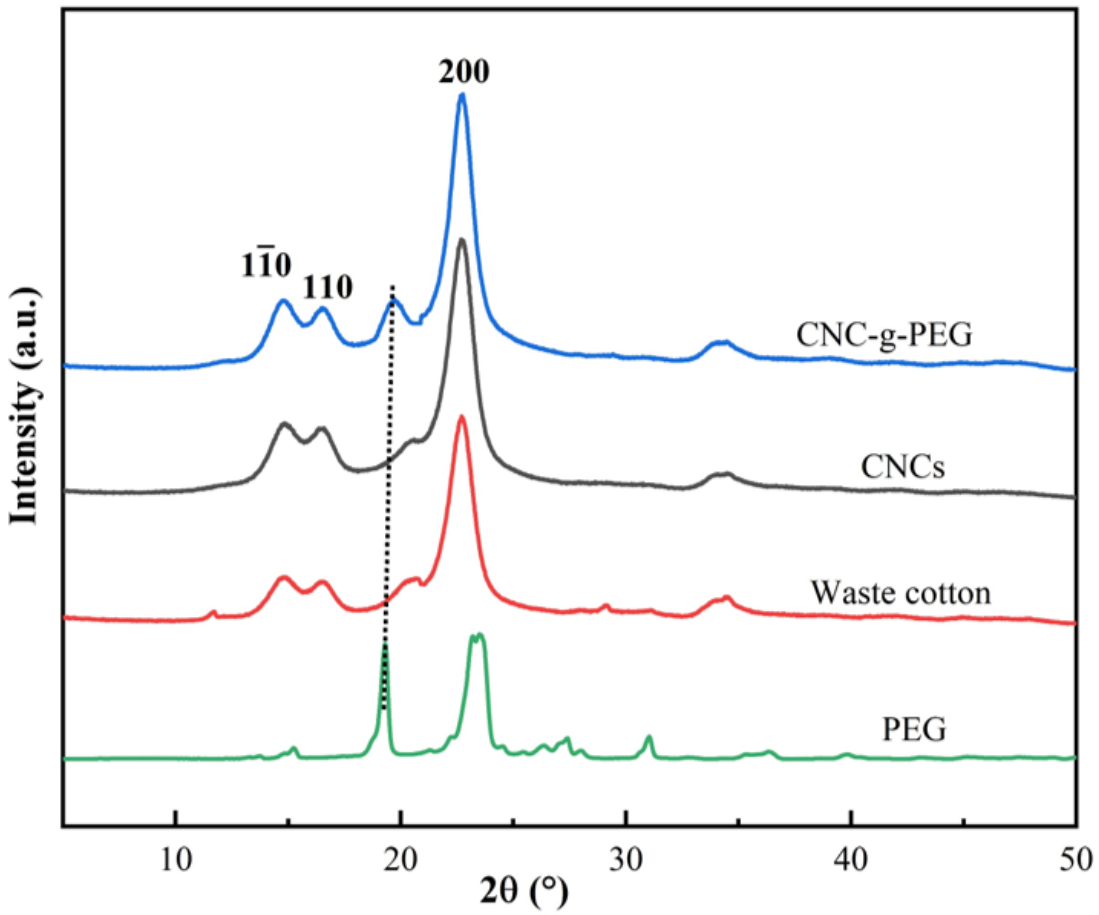

Figure 4

XRD patterns of waste cotton, PEG, CNCs, and CNC-g-PEG

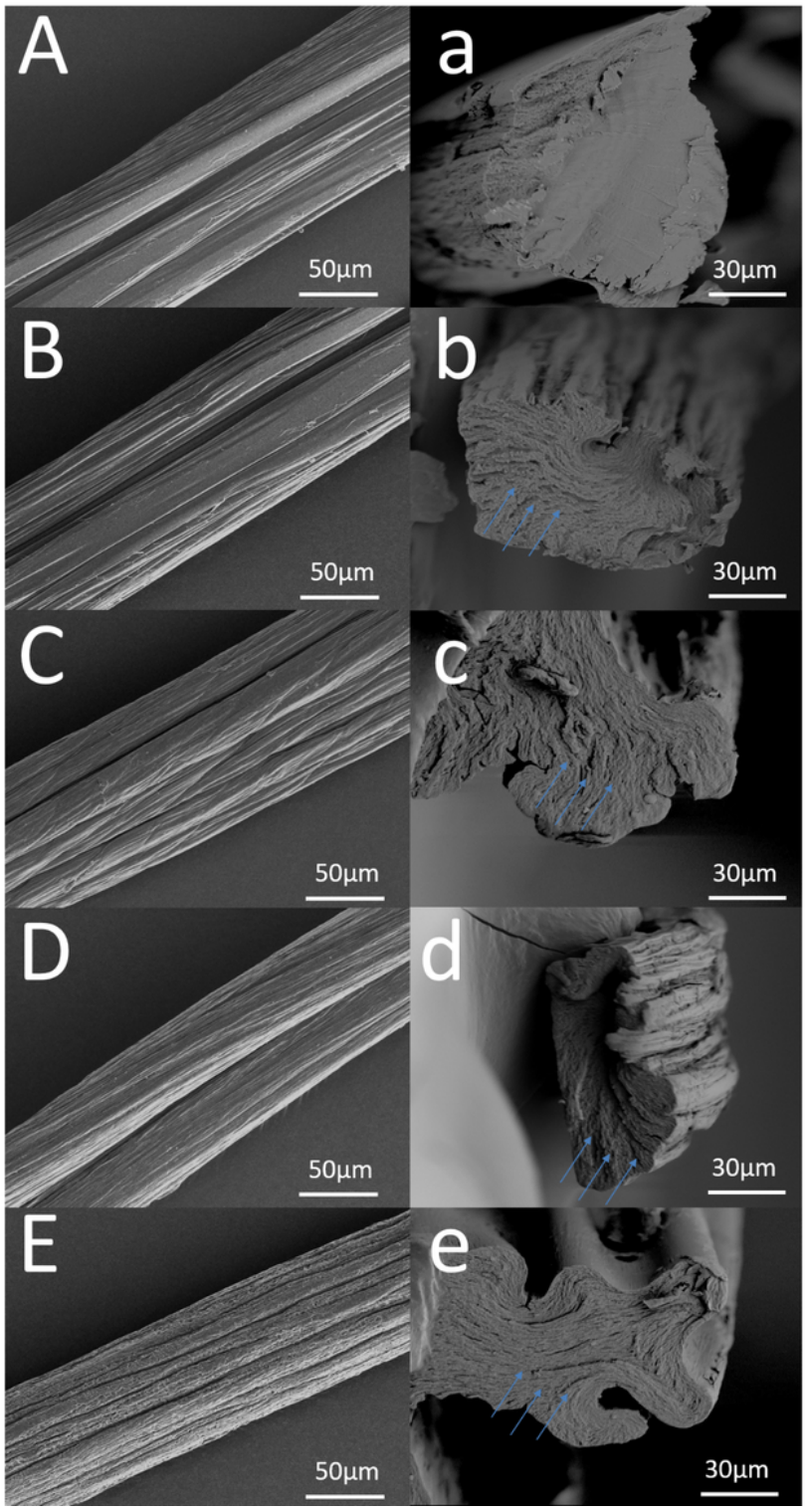

Figure 5

SEM images of Alginate fibers (A, a), CNC/Alginate fibers (B, b), CNC-g-PEG1000/Alginate fibers (C, c), CNC-g-PEG2000/Alginate fibers (D, d) and CNC-g-PEG4000/Alginate fibers (E, e)

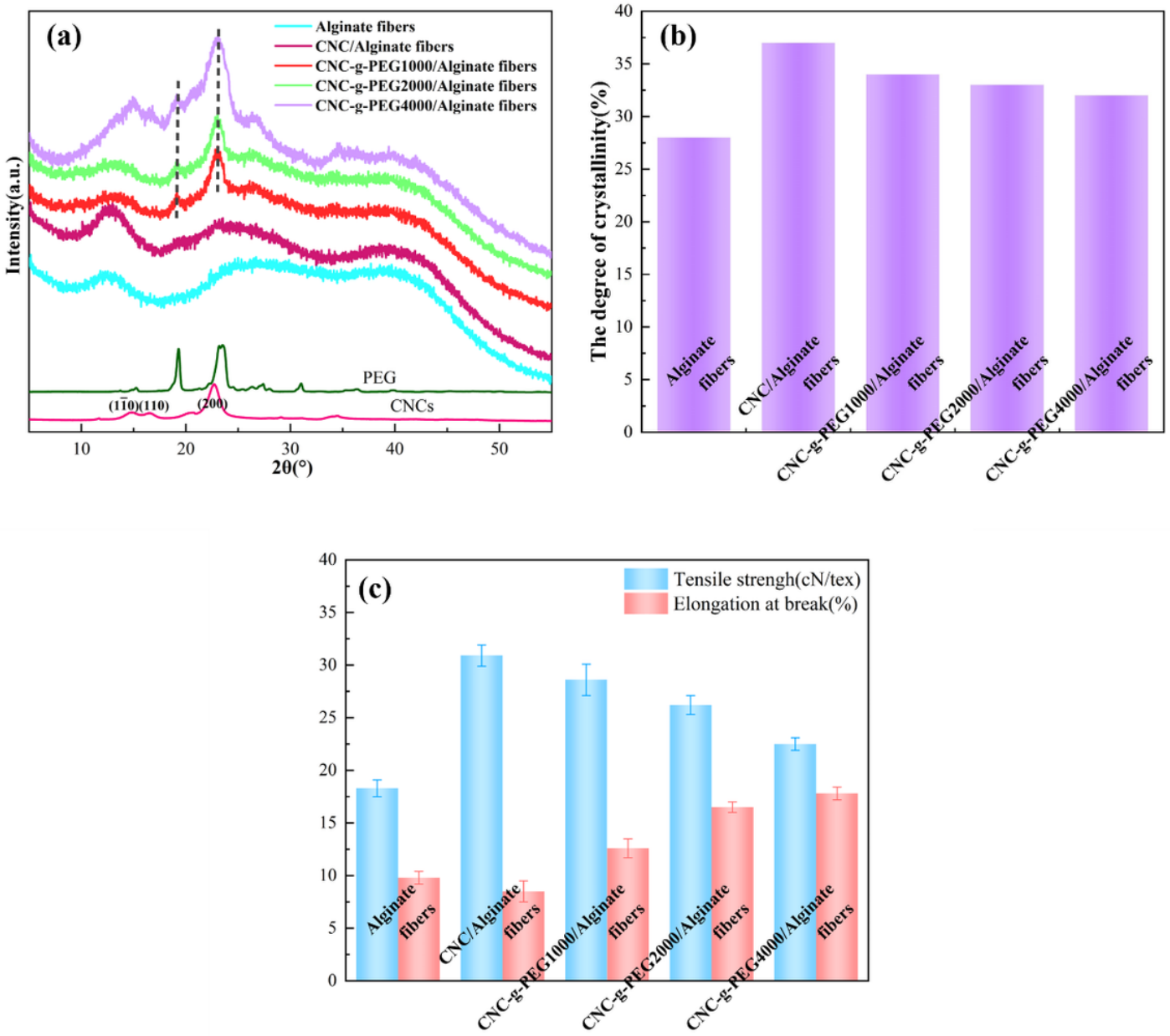

Figure 6

XRD patterns of CNCs, PEG, and the alginate composite fibers (a), Xc (b) and the tensile properties (c) of the alginate composite fibers

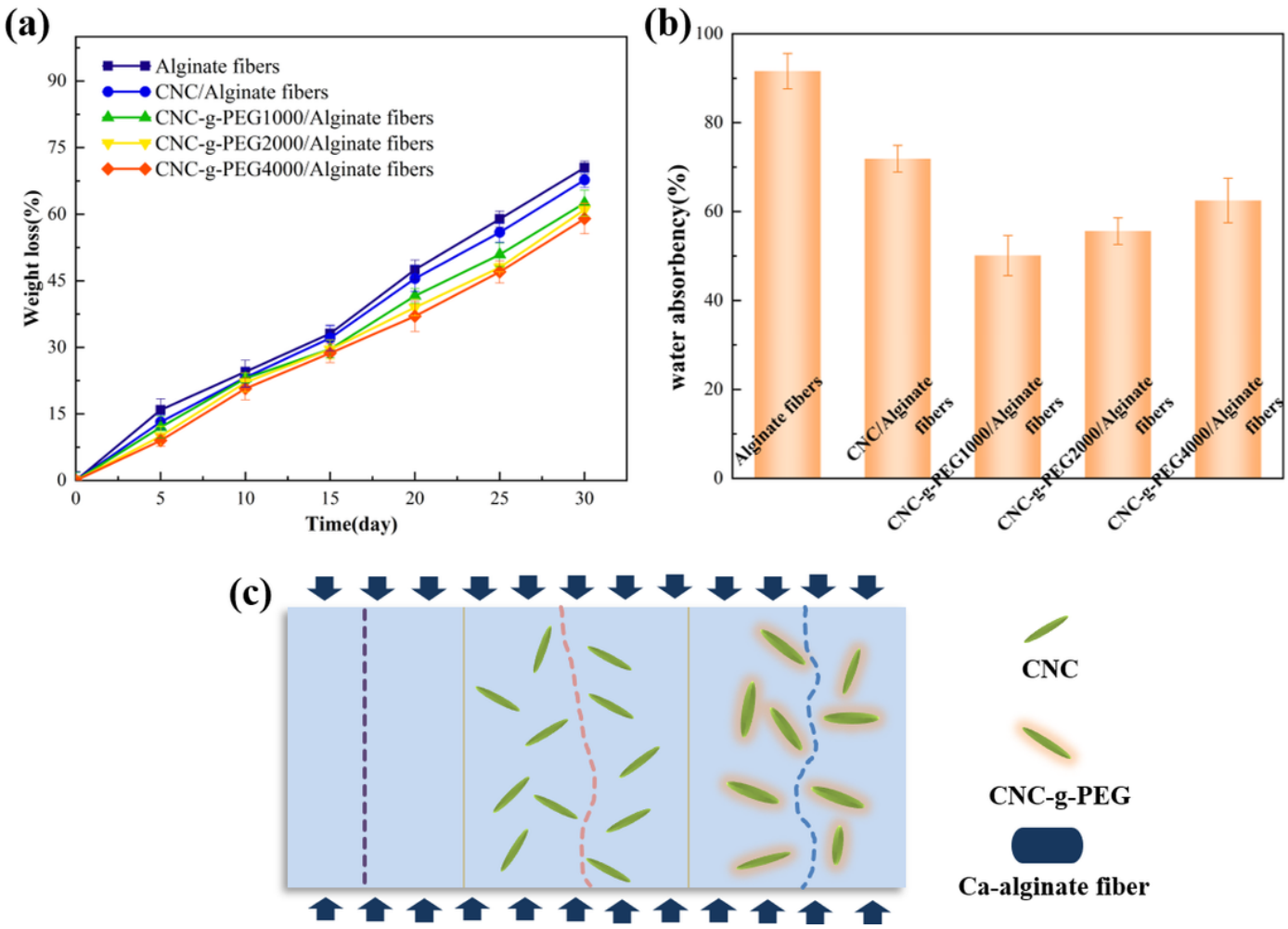

Figure 7

The weight loss rate of the alginate composite fibers in the PBS solution (a), water absorption of the alginate composite fibers (b), the penetration paths of water molecules for pure alginate fibers and the alginate composite fibers(c)

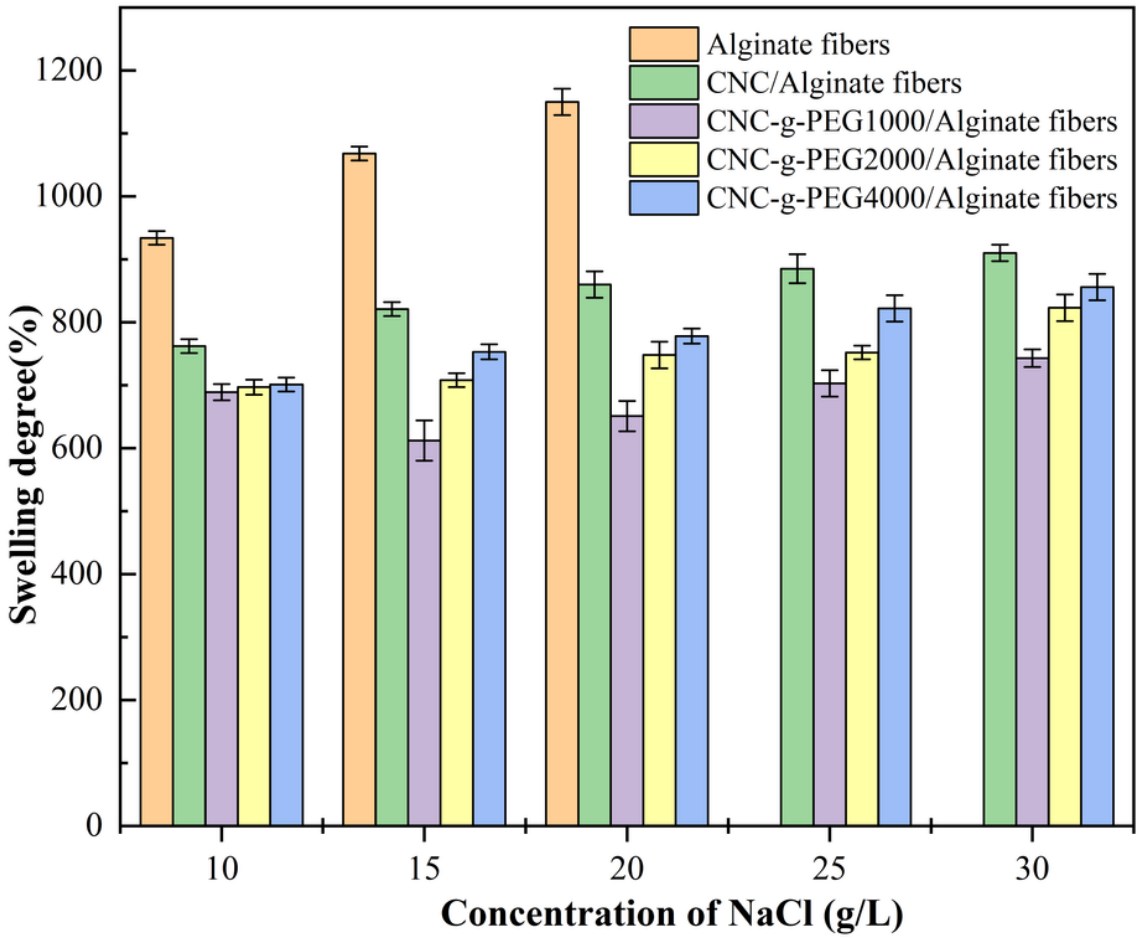

Figure 8

Salt tolerance properties of the alginate composite fibers

Supplementary Files

This is a list of supplementary files associated with this preprint. Click to download.

- Graphicalabstract.png